

Galvanostatic Growth of Passivating Films Under Transient Conditions. I. Model and Quantitative Analysis for the Zn/ZnO System

C.V. D'Alkaine*, M.A.C. Berton, P.C. Tullio

Group of Electrochemistry and Polymers, DQ-UFSCar- 13565-905 São Carlos (SP), Brazil

Received 25 September 2002; accepted in revised form 13 December 2002

Abstract

On the basis of an ohmic model and a Tafel equation describing relations between current density and overpotentials in the film and at the metal/film interface, respectively, it is shown that a quantitative analysis of galvanostatic transients for the growth of passivating ultra-thin films on the so-called non-noble metals can be obtained. As an example, the growth of ZnO on Zn in a boric/borate buffer solution is considered. In this case, the values of the transfer coefficient and the exchange current density of the reaction at the metal/film interface were found to be 1.2 and 0.11 mA cm⁻², respectively. It was shown that a single, first film occurred at low current densities and two films at high ones. The ionic resistivity inside the single, first film, during the transients, has an initial constant value region followed by a final increase indicating the aging process. For this variation the evolution of the point defect concentrations is taken into account. For the variation of the ionic resistivity with the galvanostatic current density two types of behaviors were found, depending on the current density. An interpretation of these results is advanced in terms of the concentrations, mobilities and recombination rate of point defects inside the film.

Keywords: passivation kinetics, ultra-thin films, galvanostatic experiments, quantitative analysis, zinc.

* Corresponding author. E-mail address: dalkaine@dq.ufscar.br

Introduction

Studies published on galvanostatic growth of passivating films on metals can be divided between those concerned with active/passive transitions (or prepassive regions) and those that refer to the growth of a continuous film. Both of these kind of situations depend on the metal under study, the growth conditions, the solution used and the procedure for preparation of the electrode.

For galvanostatic active/passive transitions the quantitative analysis made by Ashworth and Fairhurst [1] considers a dissolution-precipitation mechanism, following the description made by Delahay [2]. They incorporate Dignam and Gibbs' treatment [3] based on nucleation and growth concepts.

Papers concerning the quantitative analysis of galvanostatic growth of continuous films refer, in general, to quasi-stationary conditions of valve metals at high overpotentials [4-12]. Mainly they use the well-known high field ionic transport model (Hopping Motion model), which may allow for the incorporation of a concentration gradient [6].

One of the hypotheses used in these approaches is to treat the parameters in the equations as constant, as if the passivating films were not changing, so that, applications of these models tend to be valid only for stationary conditions [9] and not for transient ones where the parameters would vary. During transient growth, films are likely to be changing in structure, number of point defects and properties, basically because there has not been time enough for the film to stabilize under the chosen growth conditions. The transient situation is typical of the initial moments of film growth. At this stage two kind of films can be considered: ultra-thin films where the defect concentrations can be assumed practically homogeneous, at least to a first approximation, and thin films where concentration gradients of defects can be important. The present paper will be dedicated to the first ones.

When the measurements are made at high overpotentials, the overpotentials at the metal/film and/or the film/solution interfaces can be disregarded or, in the case of galvanostatic growth, considered constant [9]. Again, this may not be the case during a transient at low overpotentials. Here, the metal/film overpotential

must be taken into account, even for galvanostatic measurements, if it is wished to compare results at different current densities. On the other hand, the overpotential at the film/solution interface can be maintained constant when oxides are grown and the experiments are done under constant superficial pH [13,14].

Furthermore, galvanostatic transients cannot always be interpreted in terms of the Hopping Motion model. Dignam [9] has proposed that there are “battery” metals, such as Ag, Cd or Pb, for which, even accepting some experimental error, it is not possible to describe their growth in terms of the high field mechanism. Even bismuth, although a valve metal, seems to be a special case. Its special behavior in galvanostatic transients [15], seems to be related to the appearance of a space charge inside the film.

In the case of low overpotentials in ultra-thin or thin films in non-noble metals, at the initiation of growth, it may not be possible to consider the films as simple covalent, stoichiometric and crystalline solids, but rather as having a significant water content given amorphous structures [16-18]. Owing to this fact, for films in their initial stages under transient growth, the model proposed in the present paper will assume that the current density/overpotential relation inside the films follows an ohmic rather than a Hopping Motion model. It must be pointed out that this model is not conceived as an approximation of the Hopping Motion model, valid for low fields, as has been proposed [19,20]. In fact, in the present case, the ohmic relation will be assumed to apply even at high fields.

To exemplify the application of the equations of the model, the growth of ZnO on Zn in boric/borate solution was chosen. In a previous paper [21] on potentiostatic growth in the same system, the current interpretation in the literature of the composition and characteristics of the growing film was examined.

From a galvanostatic point of view, there are studies in sulfuric acid [22], in alkaline solutions [23-28], sodium carbonate and bicarbonate solutions [29] and phosphate buffer solutions [30,31] and even in sodium borate solutions [32].

Model for Ultra-thin Films and Methods of Calculation of Parameters

During the galvanostatic growth of a passivating film under convenient conditions, it will be supposed an initial homogeneous film thickness completely covering the electrode, where the potential (E) is related to the various overpotentials by [14,33]:

$$E = \eta_{m/f} + \eta_f + E_F \quad (1)$$

where $\eta_{m/f}$ and η_f are the overpotentials at the metal/film and through the film, respectively, and E_F is the Flade Potential [33]. In this equation the overpotential at the film/solution interface is taken as constant (independent of the current density, i) because it is supposed that for an oxide the controlling reaction at this interface is the O^{2-}/H_2O reaction, which can be considered practically in equilibrium in the passivity region, as long as the pH of the solution can be assumed constant [13,14] and the dissolution current can be disregarded [34]. This overpotential ($\eta_{f/s}$) is thus included in E_F in eq. (1).

Differentiating eq. (1) gives:

$$\left(\frac{\partial E}{\partial t}\right)_X = \left(\frac{\partial \eta_{m/f}}{\partial t}\right)_X + \left(\frac{\partial \eta_f}{\partial t}\right)_X \quad (2)$$

where t is the time and X can be any of the variables (E , i , etc.).

At the metal/film interface, considering an activated control, the relation between i and $\eta_{m/f}$ is given by

$$i = i_{m/f}^0 \left[\exp(\alpha_{m/f} f \eta_{m/f}) - \exp(-((z - \alpha_{m/f}) f \eta_{m/f})) \right] \quad (3)$$

where $i_{m/f}^0$ and $\alpha_{m/f}$ are the exchange current density and the anodic transfer coefficient, respectively, f is given by F/RT and z is the charge on the metal ion.

For galvanostatic conditions ($i = i_g$, the galvanostatic current density)

$$\left(\frac{\partial \eta_{m/f}}{\partial t}\right)_{i_g} = 0 \quad (4)$$

Then from eq. (2), for any region of the galvanostatic experiment where eq. (1) is valid,

$$\left(\frac{\partial E}{\partial t}\right)_{ig} = \left(\frac{\partial \eta_f}{\partial t}\right)_{ig} \quad (5)$$

For an ohmic model, the relation between i and η_f inside the film is given by

$$\eta_f = V_f \rho_f q_f i \quad (6)$$

where V_f and q_f are the volume per unit charge and the charge density (charge per unit area) of the growing film and ρ_f is its ionic specific resistivity. In general, q_f is related to i_g by

$$q_f = q_{galv} + q_0 = i_g t + q_0 \quad (7)$$

where q_0 is the charge density related to the amount of film initially present on the metal surface at the start of the electrochemical experiment and q_{galv} is the charge density related to the amount of film which has grown during the anodic galvanostatic transient. For this equation to hold, the experiments must be done in a solution in which the current efficiency can be considered as practically 100% and, consequently, virtually no dissolution current of the film needs to be considered when compared with i_g .

Under these conditions, from eqs. (5), (6) and (7) is obtained:

$$\left(\frac{\partial E}{\partial t}\right)_{ig} = V_f \rho_f i_g^2 + V_f q_f i_g \left(\frac{\partial \rho_f}{\partial t}\right)_{ig} \quad (8)$$

where V_f has been considered constant [14].

If V_f is calculated from $M_{ox}/zF\delta_{ox}$, where M_{ox} and δ_{ox} are the molecular weight and density of the film, respectively, and if, in some region of the galvanostatic E/t transient curve, $(\partial \rho_f / \partial t)$ can be taken as zero (ρ_f constant, a minimum or a maximum), then, at that point or region the ionic specific resistivity (ρ_f^*) can be calculated as

$$\rho_f^* = \frac{1}{V_f i_g^2} \left(\frac{\partial E}{\partial t}\right)_{ig, \rho_f} \quad (9)$$

From a theoretical point of view a region in which $(\partial \rho_f / \partial t)$ is zero should exist for an ultra-thin film. The reason is that the injection of point defects at the beginning (due to the passage of current through the initial film) will increase the defect concentration, while at the same time this increase will provoke a rise in

their possible recombination rates leading to a reduction in their concentrations, which will be also the result of the film growth. As a consequence, as the ionic resistivity is related with the reciprocal of the defect concentration, it must pass through a minimum or a plateau during the transient, giving rise to an inflection point or a linear region of the E/t plot in the galvanostatic transient.

From an experimental point of view the analysis above is in agreement with the fact that in a galvanostatic transient, $(\partial E/\partial t)$ always passes through a minimum or a constant region, so that, there is an inflection point or a plateau in the E/t plots. This minimum or constant region will be related, from the analysis above, with $(\partial \rho_f/\partial t)$ being equal to zero. This aspect of the E/t curve allows the experimental determination of the region in which eq. (9) is valid. The consistency of this calculation must then be proved, at the end of the process, by showing that eq. (9) was applied at a minimum or a plateau of ρ_f .

It is then possible to calculate η_f^* from eq. (6), for the inflection point or plateau region, by inserting ρ_f^* as the value of ρ_f . From eqs. (6) and (9):

$$\eta_f^* = \frac{\left(\frac{\partial E}{\partial t}\right)^*}{i_g} q_f^* \quad (10)$$

where $(\partial E/\partial t)^*$ and q_f^* must also be determined at the special point under consideration.

With these η_f^* values it is possible to determine the values of $(E - \eta_f)$ for each i_g , that is, the potential corrected by the ohmic drop through the film. By eq. (1) these values are the values of $(E_F + \eta_{m/f})$ for each i_g . The value of $(E_F + \eta_{m/f})$, for a given i_g , is constant during a galvanostatic transient. Thus, it is now possible to calculate η_f for any position on the galvanostatic curve, not only that for which eq. (9) is valid. To clarify this statement, in Fig. 1 is shown a theoretical transient galvanostatic curve for a given i_g together with the E_F and the corresponding $(E_F + \eta_{m/f})$ value. On the same plot, some values of the various film overpotentials at different times (t) are plotted.

Finally, an interesting point that could verify the correctness of the analysis above is related to the plot of $\log i_g$ versus $(E - \eta_f)$ or $(E_F + \eta_{m/f})$, using the data obtained by eq. (9). If eq. (3) is valid, this plot should be a normal Tafel plot like those for reactions in solution. Far from E_F , it must give a straight line and near E_F , owing to the presence of the inverse reaction, it must tend to $-\infty$. From such a plot it would be possible to determine experimentally E_F , if sufficient small values of i_g are used. By extrapolation of the straight line region to E_F , $i_{m/f}^0$ will be obtained. From the slope of the straight line region, the transfer coefficient of the corresponding reaction will be obtained.

An important aspect of this Tafel plot is that it permits the evaluation of q_0 , as will be seen in the analysis of the results.

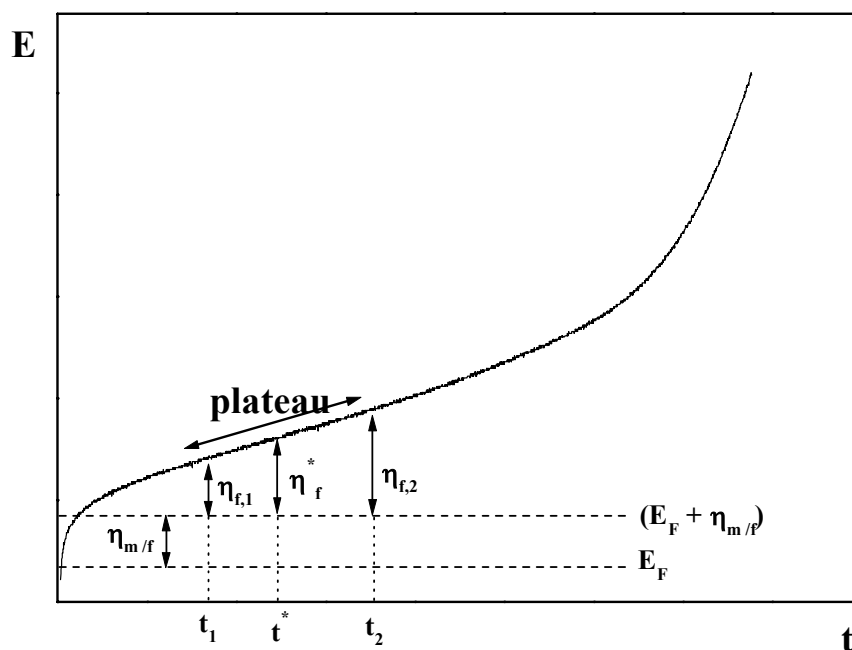


Figure 1. Schematic anodic galvanostatic curve showing E_F , the constant $\eta_{m/f}$ and various η_f values. Also indicated on the E/t curve is the plateau region in which eq. (10) can be applied.

Experimental

The working electrode was 99.99% pure Zn from Aldrich, embedded in an epoxy resin, with an electroactive disk surface area of 0.22 cm^2 . This electrode was polished with 600 emery paper before each measurement.

The reference electrode to which all potentials are referred to was Hg/HgO/1.0 M KOH solution.

The electrolyte solution was 0.3 M H_3BO_3 plus 0.15 M $\text{Na}_2\text{B}_4\text{O}_7 \cdot 10\text{H}_2\text{O}$ deoxygenated by N_2 bubbling. The reagents were PA and the water thrice distilled. Calculations show that this buffer solution maintains the pH at the electrode surface constant, even during the film growth. This is important for the constancy of $\eta_{f/s}$.

In all experiments the procedure was as follows: the working electrode was introduced into the solution, immediately after polishing, at a cathodic current density of 0.13 mA cm^{-2} (real area), maintained at this current density until the potential reached -1.335 V , when the current density was changed to the corresponding anodic i_g to initiate the growth. Only the first transient growth was registered and then the electrode was polished again and the process repeated.

All the current and charge densities are expressed in terms of the working electrode real area. To obtain this area, the roughness factor (r) of the working electrode, after polishing, was determined by comparing the charge involved in an anodic passivating voltammetric peak for this electrode, for a given sweep velocity (v of 20 mV s^{-1}), with that of a standard Pt electrode of known real area covered with a layer of Zn, uniform and very thin in thickness (a Pt/Zn electrode). Both measurements were done in the same deoxygenated solution (0.5 M NaHCO_3). The data on the Pt/Zn electrode with known real area used as a standard were obtained by Mascaro [35]. This Pt/Zn standard electrode was obtained by the deposition, layer by layer, of 11 mC cm^{-2} of zinc on a platinum disk electrode. The idea was that the passivating film grown on both electrodes (the working and the Pt/Zn) was the same and the ratio between their experimental peak charge densities was thus proportional to the ratio of real areas. The real area of the Pt/Zn electrode was obtained [35] by determining the

Pt electrode original area in 0.5 M H₂SO₄ solution. This was done by measuring the hydrogen adsorption peaks [36]. The 11 mC cm⁻² of Zn deposited on Pt, layer by layer, is considered not to alter the roughness factor of the Pt/Zn electrode used as reference. In the present work the roughness factor of the working electrode, after polishing with 600 emery paper, was found to be 2.3.

Results and Discussion

General Description and Initial Rise of Potential

In Figs. 2 and 3 are presented typical galvanostatic transients in the galvanostatic current regions studied. For comparison the transient at 0.39 mA cm⁻² has been plotted in the two figures.

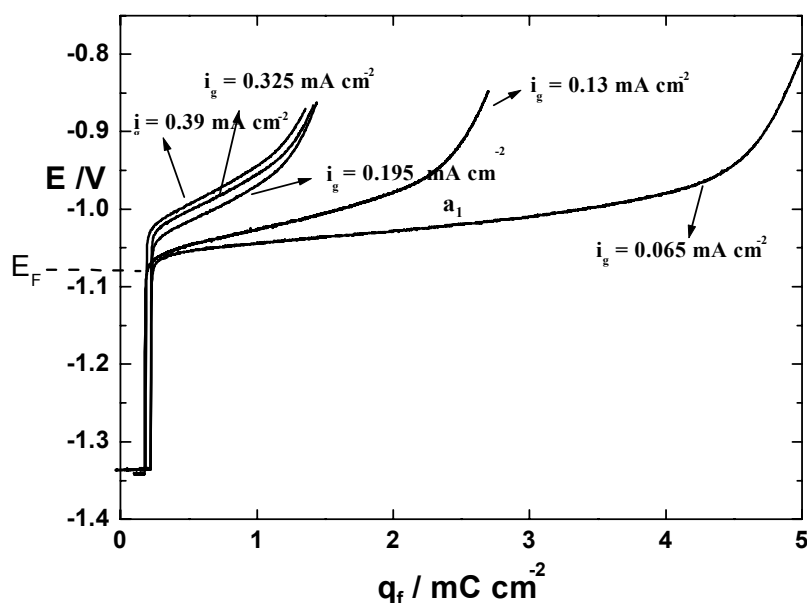


Figure 2. Typical experimental galvanostatic anodic transients for the growth of ZnO on Zn at various current densities indicated in the figure. The results correspond to the lower current densities studied. a_1 in the figure indicates the potential region of the first plateau. The current density was calculated taking into account the real area (roughness factor of 2.3).

As expected in this kind of galvanostatic plots, after the constant potential obtained at the initial cathodic current density, when the current density is changed to an anodic one, there is an initial region with an abrupt potential

increase, followed by a kind of arrest or plateau (with a portion with a linear relation between E and t). This plateau ends in a second increase of the potential. For higher current densities (Fig. 3), a second plateau appears at higher potentials, with its corresponding linear region. The two plateaux have different slopes. The potential of the first linear region, taken at its middle, lies between approximately -1.05 V and -0.8 V, depending on the i_g , while that

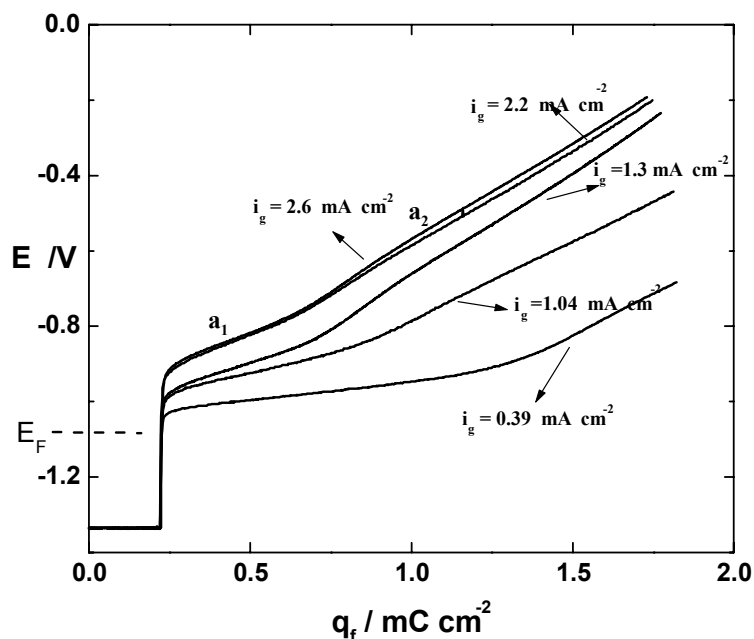


Figure 3. Typical experimental galvanostatic anodic transients for the growth of ZnO on Zn at various current densities indicated in the figure. The results correspond to the higher current densities studied. a_1 in the figure indicates the potential region of the first plateau and a_2 that of the second. The current density was calculated taking into account the real area (roughness factor of 2.3).

of the second varies between approximately -0.65 V and -0.35 V. These two plateaux indicate the existence of two films, designated a_1 and a_2 . These two films have been reported previously [21] from potentiostatic growths.

The initial abrupt increase in potential for values $E < E_F$ is the result of charging of the metal/initial film/solution interface, together with the reduction of water, this last one only at the beginning. When the potential becomes higher than E_F , the growth of the film starts, reducing the current necessary for charging the

interface. In this situation the system arrives at a condition in which the charging current becomes negligible compared with the current used for the growth of the film, due to the thickening of this last one. Following this evolution, the system arrives at the plateau region. Calculations of the capacity values at different i_g for $E < E_F$, taken into account the hydrogen evolution, gave $17 \pm 4 \mu\text{F cm}^{-2}$, given a relative dielectric constant for the initial film of 3.2. This value was calculated using a value for the charge density of the initial film (its thickness), which will be determined below. The relative dielectric constant obtained can be compared with that for bulk ZnO [37] of 7.9.

First Plateau Region and the Subsequent Rise in Potential

As explained in previous section, a linear region in a galvanostatic experiment, from the point of view of the equations, implies a constant ionic specific resistivity (see eqs. (1), (3), (6) and (7)).

The increase after the arrest must be attributed in this model to film aging, producing an increase in the ionic specific resistivity. Sometimes, as in the case of higher current densities in the present work, after aging of the first film, another film may be produced, giving rise to a second plateau. Nevertheless, in any case, there is always the final increase of potential, because the whole film always undergoes aging at the end of the transient.

When the experiment reaches the first plateau, it is then possible to apply the equations deduced for galvanostatic transients. This means calculating, in the first plateau region, the value of ρ_f^* , using eq. (9). Knowing this value and the charge density that has passed up to the chosen point, it is possible to correct the potential by the ohmic drop through the film (using eq. (6)). This permits the calculation of $(E_F + \eta_{m/f})$ for different i_g (using eq. (1)). It is then possible to obtain the Tafel plot at the metal/film interface. The plot of $\log i_g$ versus $(E - \eta_f)$ in the first plateau region allows the determination of the Tafel parameters at the metal/film interface.

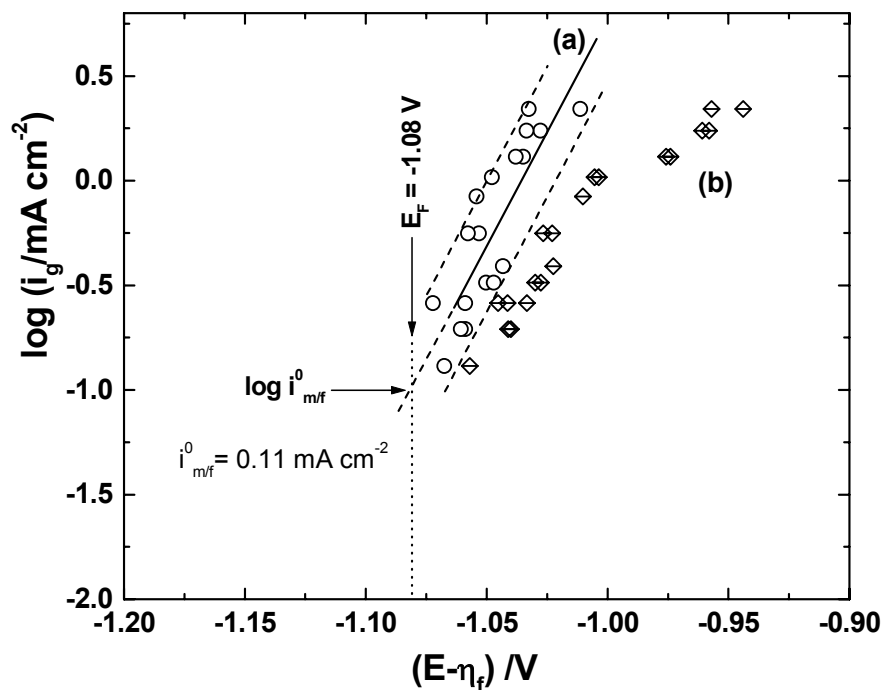


Figure 4. Tafel representation of $\log i_g$ versus E corrected for the ohmic drop through the film. This ohmic drop was calculated using eqs. (7) and (10). Curve a: $q_0 = 0.22 \text{ mC cm}^{-2}$. Curve b: $q_0 = 0.0 \text{ mC cm}^{-2}$.

For the above calculations it is necessary to know the value of q_0 (see eqs. (6) and (7)). In Fig. 4a there is the $\log i_g / (E - \eta_f)$ plot for a q_0 value of 0.22 mC cm^{-2} real area (with $r = 2.3$). This value was chosen after trials with different q_0 values. When higher q_0 values were used, the plots show a decreasing $\log i_g$ with an increasing $(E - \eta_f)$, which contradicts any physical meaning. When lower q_0 values were used, there was no linearization of the curve for the higher i_g . To illustrate this last fact, in Fig. 4b the results for zero q_0 have also been plotted.

From the plot in Fig. 4a and using the E_F value previously obtained for this system [21], it was possible to obtain the exchange current density and the transfer coefficient at the metal/film interface. The i_{mf}^0 was 0.11 mA cm^{-2} and the α_{mf} was 1.2. This last value, assuming only one step for the reaction, means that the activation energy barrier is not totally symmetric.

Using the calculated $(E_F + \eta_{m/f})$ value for each i_g , it was then possible to obtain, for any time or film charge density of each galvanostatic transient, the corresponding η_f values in the region of the first arrest, as indicated in Fig. 1. In Fig. 5, η_f results are plotted against q_f , for different i_g indicated in the figure. See that it is clear that the present work is referred to an ultra-thin film because the maximum analyzed charge density arrives only to about 5 mC cm^{-2} for the worst case.

Three galvanostatic current density regions can be defined in Fig. 5. In the first, for high i_g ($i_g > 0.325 \text{ mA cm}^{-2}$), the η_f versus q_f relation depends on i_g . The second, for intermediate i_g (between 0.325 and 0.195 mA cm^{-2}), is characterized by the fact that changes in i_g practically do not affect the η_f/q_f relation. Finally, in the third region, at low i_g (lower than 0.195 mA cm^{-2}), once more the η_f versus q_f relation becomes dependent on i_g . This shows the complexity of this kind of plots. Nevertheless, from these data for different transients, it is possible to calculate ρ_f through eq. 6 and to study its evolution not only with q_f but also with i_g . These results can be seen in Fig. 6, for high, and in Fig. 7, for low i_g . For all the galvanostatic transients, there is a plateau for ρ_f during the transient (in the linear E/t region) followed by an increase. They were always selected within these plateaux the points (arrows in Figs 6 and 7) for the application of eq. (10). From a theoretical point of view the ionic resistivity depends on the defect concentrations and the ionic mobilities. From the results of Figs. 6 and 7, in the plateaux of Figs. 2 and 3, if it is assumed that the ionic mobilities in this zone are constant, then the injection of defects must be compensated by the increase of the film thickness and the recombination process, so that the defect concentrations, and thus ρ_f , become constant.

For the final increase of ρ_f (Figs. 6 and 7), at higher q_f , beyond the plateau zone in Figs. 2 and 3, a reduction in the ionic mobility of the defects may be the explanation. With the passage of time there must be an evolution of the film structure towards a decrease in ionic mobility of the defects: the aging process of the film. This evolution can be related, for example, to dehydration.

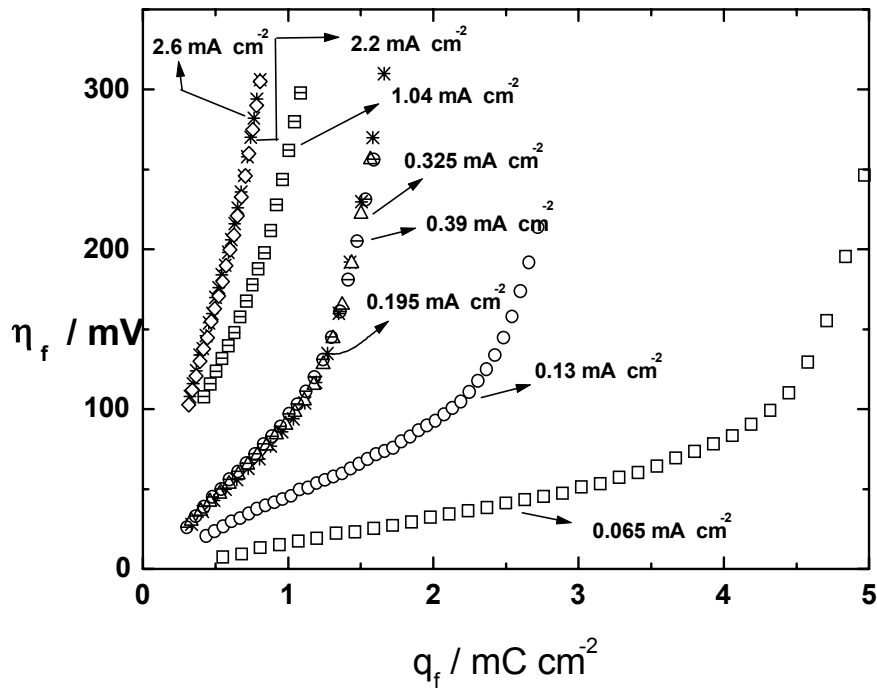


Figure 5. Plot of the calculated η_f versus q_f values for the various i_g indicated in the figure.

Finally, in Figs. 6 and 7 should be noted the variation of plateau ρ_f values, with i_g . For high i_g (Fig. 6), ρ_f decreases with i_g . On the other hand, at lower i_g (Fig. 7), as i_g increases, ρ_f increases.

From a theoretical point of view, at constant ionic mobilities, an increase of i_g implies an increase in the defect concentration and a lowering of ρ_f , when the equilibrium between the injection, the recombination and the growth of the film is attained at the plateau. Thus, the results of Fig. 6 at high i_g are in agreement with these considerations. On the other hand, in Fig. 7 (low i_g) where the ρ_f at the plateau increases with the increase of i_g , there must be some influence of a change in the constant ionic mobilities in the plateau with the change of structures generated by the change in i_g . At low i_g there will be time for transformations in the film to give rise to changes in the constant ionic mobilities in the plateau region. It seems that the aging implies a decrease in the mobilities perhaps related, as has been pointed out before, with the dehydration of the film.

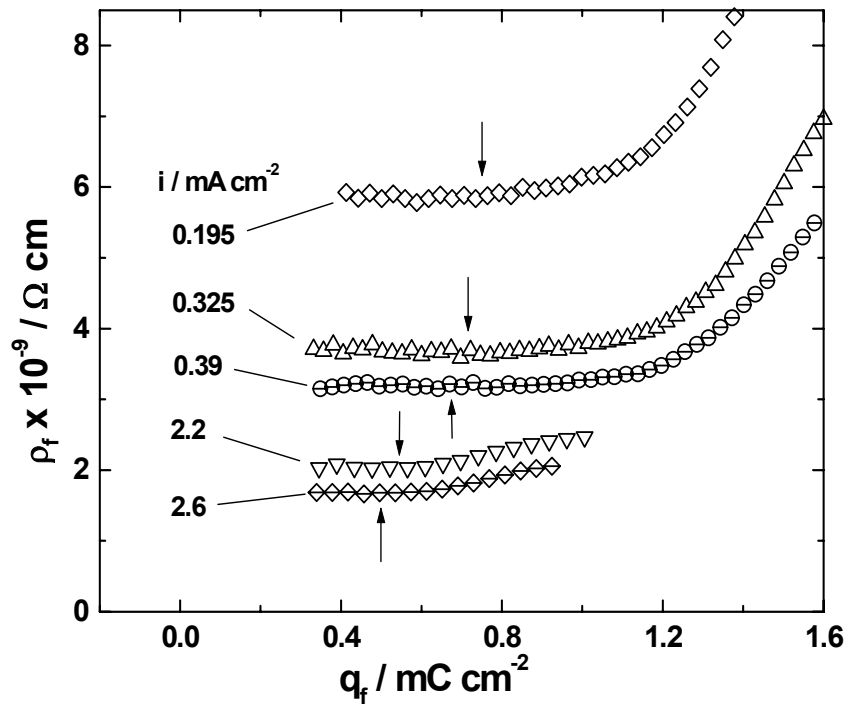


Figure 6. Plot of calculated ρ_f versus q_f for the various i_g indicated in the figure. High galvanostatic current densities.

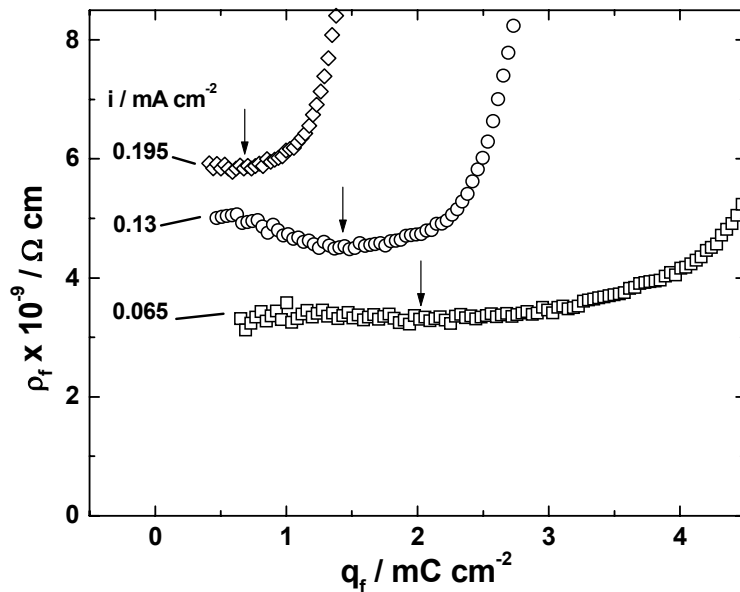


Figure 7. Plot of calculated ρ_f versus q_f for the various i_g indicated in the figure. Low galvanostatic current densities.

Conclusions

On the basis of an ohmic model for the relation between current density and overpotential through the film and a Tafel equation relating current density and overpotential at the metal/film interface, it is shown that a complete quantitative analysis of the galvanostatic transient growth of ultra-thin passivating films on the so-called non-noble metals is possible. To demonstrate this, the case of the growth of ZnO on Zn in a buffer of boric/borate solution has been examined.

The theoretical analysis of the results enables the ionic specific resistivity of the film to be calculated during the transient growth. This quantity is constant during the E/t plateau and rises at its end. A proposition is advanced to explain these results on the basis of the concentration and mobility of point defects inside the film. The practically constant ionic specific resistivity of the plateau region of the transient is interpreted as a constant ionic mobility and concentration of defects inside the film. The increase of the ionic resistivity at the end of the transients is explained in terms of the reduction of the ionic mobility of the defects, due to changes in the film structure with aging. At low current densities, it is found that even on the plateau it is possible that some modifications of the film occur, changing the values of constant mobilities at these regions, with i_g .

The equations also allow the calculation of the current density/overpotential relation at the metal/film interface. The calculations afford not only a determination of the initial amount of film at the beginning of the experiments, for the initial selected conditions, but also the corresponding transfer coefficient and exchange current density of this process at this interface. The $\alpha_{m/f}$ was 1.2 and the $i_{m/f}^0$ 0.11 mA cm⁻². The initial charge density results to be 0.22 mC cm⁻² for the selected initial conditions.

Finally, it is proposed that the initial evolution of the potential in the galvanostatic transient, for potentials lower than the Flade potential, is the result of charging of the metal/initial film/solution interface, in parallel, at the start, with the hydrogen evolution reaction. Hence, it was possible to calculate the relative dielectric constant of the initial film. It gave 3.2. With the increase of

film thickness, arriving to the plateau, the charging current diminishes so much that the whole current goes practically only to grow the film.

Acknowledgments

The authors are grateful to FAPESP for the financial support for the program to which the present paper belongs. Two of the authors (M. A. C. B. and P.C. T.) are grateful to CNPq for their Ph.D. scholarships.

References

1. V. Ashworth, D. Fairhurst, *J. Electrochem. Soc.* 124 (1977) 506.
2. P. Delahay, *New Instrumental Methods in Electrochemistry*, John Wiley & Sons, New York (1964).
3. M.J. Dignam, D.B. Gibbs, *Can. J. Chem.* 48 (1970) 1242.
4. D.A. Vermilyea, in *Advances in Electroch. and Electroch. Eng.* (Edited by P. Delahay, C.W. Tobias), Vol. 3, Chap. 4, Interscience, New York (1963).
5. M.J. Dignam, in *Oxide and Oxide Films* (Edited by J.W. Diggle and A.K. Vijh), Vol. 1, p. 91, Marcel Dekker Inc., New York (1972).
6. A.T. Fromhold Jr, in *Oxide and Oxide Films* (Edited by J.W. Diggle, A.K. Vijh), Vol. 3, p. 1, Marcel Dekker Inc., New York (1976).
7. C.J. Dell'Oca, D.L. Pulfrey, L. Young, *Phys. Thin Films* 6 (1971) 1.
8. F. Di Quarto, A. Di Paola, C. Sunseri, *J. Electroch. Soc.* 127 (1980) 1016.
9. M.J. Dignam, in *Comprehensive Treatise of Electrochemistry* (Edited by J.O'M. Bockris, B.E. Conway, E. Yeager, E. White), Vol. 4, p. 247, Plenum Press, New York (1981).
10. T. Hurlen, *Electroch. Acta* 39 (1994) 2125.
11. T. Hurlen, E. Gulbrandsen, *Electroch. Acta* 39 (1994) 2169.
12. M. Metikos-Hukovic, A. Resetic, V. Gvozdic, *Electroch. Acta* 40 (1995) 1777.
13. N. Sato, *J. Electroch. Soc.* 129 (1982) 255.
14. C.V. D'Alkaine, L.M.M. de Souza, F.C. Nart, *Corrosion Science* 34 (1993) 129.

15. D.E. Williams, *Electroch. Acta* 27 (1982) 411.
16. M.H. Dean, U. Stimming, *Corrosion Science* 29 (1989) 199.
17. J.O'M Bockris, *Corrosion Science* 29 (1989) 291.
18. H. Gerisher, *Corrosion Science* 31 (1990) 81.
19. M. Bojinov, I. Kanazirskj, A. Girginov, *Electroch. Acta* 40 (1995) 873.
20. D.E. Williams, G.A. Wright, *Electroch. Acta* 21 (1976) 1009.
21. C.V. D'Alkaine, M.N. Boucherit, *J. Electrochem. Soc.* 144 (1997) 3331.
22. H. Krhon, S. Rashwan, F. Back, *Ber. Bunsenges. Phys. Chem.* 95 (1991) 61.
23. T.P. Dirkse, *J. Electrochem. Soc.* 125 (1978) 1591.
24. J. Hendriks, A. Van Der Putten, W. Visscher, E. Barendrecht, *Electroch. Acta* 29 (1984) 81.
25. M. Liu, G.M. Cook, N.P. Yao, *J. Electrochem. Soc.* 128 (1981) 1663.
26. S. Szpak, C. J. Gabriel, *J. Electrochem. Soc.* 126 (1979) 1914.
27. Y. Chang, G. Prentice, *J. Electrochem. Soc.* 131 (1984) 1465.
28. K. Bass, P.J. Mitchell, G.D. Wilcox, J. Smith, *J. Power Sources* 39 (1992) 273.
29. H. Kaesche, *Electroch. Acta* 9 (1964) 383.
30. C.P. Pauli, O.A.H. Derosa, M.C. Giordano, *J. Electroanal. Chem.* 86 (1978) 335.
31. C.P. Pauli, M.C. Giordano, H.T. Mishima, *J. Electroanal. Chem.* 103 (1979) 95.
32. E.E. Abd El Aal, *Corrosion* 55 (1999) 583.
33. K.J. Vetter, *Electrochemical Kinetics. Theoretical and Experimental Aspects*, p. 761. Academic Press, New York (1967).
34. K.J. Vetter, F. Gorn, *Electroch. Acta* 18 (1973) 321.
35. L.H. Mascaro, Ph.D. Thesis, Chemistry Program, São Carlos Federal University, São Carlos (SP), Brazil (1992).
36. S. Trasatti, O.A. Petrii, *Pure and Applied Chem.* 63 (1991) 711.
37. Y. Pleskov, Y.Y. Gurevich., *Semiconductor Photoelectrochemistry*, p. 349. Consultant Bureau, New York (1986).